

G-protein–coupled formyl peptide receptors play a dual role in neutrophil chemotaxis and bacterial phagocytosis

Xi Wen^a, Xuehua Xu^a, Wenxiang Sun^b, Keqiang Chen^c, Miao Pan^a, Ji Ming Wang^c,
Silvia M. Bolland^b, and Tian Jin^{a,*}

^aChemotaxis Signal Section and ^bAutoimmunity and Functional Genomics Section, Laboratory of Immunogenetics, National Institute of Allergy and Infectious Diseases, National Institutes of Health, Bethesda, MD 20852; ^cCancer and Inflammation Program, Center for Cancer Research, National Cancer Research Institute at Frederick, Frederick, MD 21702-1201

ABSTRACT A dogma of innate immunity is that neutrophils use G-protein–coupled receptors (GPCRs) for chemoattractant to chase bacteria through chemotaxis and then use phagocytic receptors coupled with tyrosine kinases to destroy opsonized bacteria via phagocytosis. Our current work showed that G-protein–coupled formyl peptide receptors (FPRs) directly mediate neutrophil phagocytosis. Mouse neutrophils lacking formyl peptide receptors (Fpr1/2^{-/-}) are defective in the phagocytosis of *Escherichia coli* and the chemoattractant N-formyl-Met-Leu-Phe (fMLP)-coated beads. fMLP immobilized onto the surface of a bead interacts with FPRs, which trigger a Ca²⁺ response and induce actin polymerization to form a phagocytic cup for engulfment of the bead. This chemoattractant GPCR/Gi signaling works independently of phagocytic receptor/tyrosine kinase signaling to promote phagocytosis. Thus, in addition to phagocytic receptor-mediated phagocytosis, neutrophils also utilize the chemoattractant GPCR/Gi signaling to mediate phagocytosis to fight against invading bacteria.

Monitoring Editor

Peter Van Haastert
University of Groningen

Received: Jun 12, 2018

Revised: Dec 6, 2018

Accepted: Dec 6, 2018

INTRODUCTION

Phagocytosis by human neutrophils is an essential part of innate immunity for fighting against bacterial infections (Underhill and Ozinsky, 2002; Underhill *et al.*, 2016; Freeman and Grinstein, 2014a). On bacterial infection, neutrophils leave the bloodstream and migrate to infection sites to eliminate bacterial pathogens (Nathan, 2006; Lammermann *et al.*, 2013; Shelef *et al.*, 2013; Kovacs *et al.*, 2014). Neutrophils chase bacteria by detecting gradients of chemoattractants derived from bacteria and migrating toward them via

chemotaxis (Majumdar *et al.*, 2016). Once reaching the infection site, neutrophils catch and engulf bacteria via phagocytosis. Phagocytosis consists of the following steps: 1) receptors recognize and bind specific ligands on the bacterial surface; 2) activation of receptors mediates reorganization of actin cytoskeleton, which induces phagocytic cup formation for bacterial engulfment; 3) phagosomes with internalized bacteria fuse with lysosomes to form phagolysosome where bacteria are digested (Nathan, 2006; Swanson, 2008; Bestebroer *et al.*, 2010; Amulic *et al.*, 2012). The current paradigm is that neutrophils use G-protein–coupled receptors (GPCRs) to detect chemoattractants derived from infection sites and to migrate toward bacteria and then switch to phagocytic receptors to bind opsonized bacteria for phagocytosis (Michl *et al.*, 1979; Bestebroer *et al.*, 2010). Specifically, chemoattractant GPCRs linked to heterotrimeric Gi proteins trigger the activation of intracellular signal transduction pathways that ultimately regulate the spatiotemporal organization of the actin cytoskeleton necessary for cell migration (Jin *et al.*, 2008; Huang *et al.*, 2013; Hoeller *et al.*, 2016; Woodham *et al.*, 2017). However, phagocytic receptors, including those for complements and immunoglobulin G (IgG) and several scavenger receptors, bind ligands on the bacterial surface and activate tyrosine kinases to promote actin polymerization for the engulfment of the

This article was published online ahead of print in MBoC in Press (<http://www.molbiolcell.org/cgi/doi/10.1091/mbc.E18-06-0358>) on December 12, 2018.

Author contributions: Conceptualization, T.J. and X.W.; methodology, X.W. and M.P.; investigation, X.W., W.S., and X.X.; resources, K.C., J.W., and S.B.; writing, T.J., X.W. and M.P.; supervision, T.J.

*Address correspondence to: Tian Jin (tjin@niaid.nih.gov).

Abbreviations used: ACK, ammonium-chloride-potassium; DMSO, dimethyl sulfoxide; FACS, fluorescence-activated cell sorting; FITC, fluorescein isothiocyanate; fMLP, N-formyl-Met-Leu-Phe; IgG, immunoglobulin G; PP2, C₁₅H₁₆CIN₅.

© 2019 Wen *et al.* This article is distributed by The American Society for Cell Biology under license from the author(s). Two months after publication it is available to the public under an Attribution–Noncommercial–Share Alike 3.0 Unported Creative Commons License (<http://creativecommons.org/licenses/by-nc-sa/3.0>). “ASCB®,” “The American Society for Cell Biology®,” and “Molecular Biology of the Cell®” are registered trademarks of The American Society for Cell Biology.

bacteria (Underhill and Ozinsky, 2002; Canton et al., 2013; Rougerie et al., 2013; Futosi and Mocsai, 2016). However, studies in primitive phagocytes suggest that this paradigm remains incomplete. For example, *Dictyostelium discoideum* and *Drosophila* cells are primitive phagocytes that can chase bacteria via chemotaxis and ingest them via phagocytosis (Beck and Habicht, 1996; DeVries et al., 2006), but they do not have the capacity to generate either complements or IgGs for phagocytic receptors. Moreover, *D. discoideum* does not have receptor-coupled tyrosine kinases that regulate the reorganization of the actin cytoskeleton (Goldberg et al., 2006). Therefore, human phagocytes may have another mechanism to recognize and eliminate bacteria. Decades ago, it was reported that adhered neutrophils could efficiently ingest surface-associated pathogens in the absence of opsonins during the recovery from pneumococcal pneumonia (Wood et al., 1946a,b). Recent studies also showed that neutrophils from zebrafish and human can effectively engulf unopsonized microbes on tissue or on coated surfaces via phagocytosis (Colucci-Guyon et al., 2011; Lu et al., 2014). However, the molecular mechanism underlying the “surface-dependent and opsonin-independent phagocytosis” is not known.

Dictyostelium discoideum cells are professional phagocytes that pursue bacteria via chemotaxis and consume them as food through phagocytosis (Maniak et al., 1995; Cosson and Soldati, 2008; Isik et al., 2008). Similarly to neutrophils, *D. discoideum* amoeba detect chemoattractant gradient and migrate toward bacteria, followed by engulfment and ingestion of the bacteria (Pan et al., 1975, 2016; Manahan et al., 2004). Many years ago, it was discovered that *D. discoideum* amoeba are able to detect folic acid released from bacteria (Pan et al., 1972). However, the receptors for sensing folic acid and the receptors for mediating bacterial phagocytosis by *D. discoideum* had not been identified until recently. By using a newly developed quantitative phosphoproteomic method to deorphan GPCRs, we identified a GPCR (fAR1) as a folic acid-receptor in *D. discoideum* (Pan et al., 2016). We further discovered that this stereotypical phagocyte utilizes fAR1, a class C GPCR, to simultaneously detect bacteria-secreted folate for chasing bacteria and microbial-associated molecular patterns (MAMPs) and lipopolysaccharide (LPS) for engulfing and consuming them (Pan et al., 2016, 2018). Thus, this simple organism uses one chemoattractant GPCR-mediated signaling network for both “chemoattractant-mediated cell migration” to chase bacteria and “chemoattractant-mediated engulfment” to ingest them. We proposed that phagocytes of higher organisms, such as neutrophils from animals and human, may also utilize chemoattractant-mediated engulfment to promote phagocytosis of bacteria (Pan et al., 2016). Interestingly, human neutrophils use formyl peptide receptors (FPRs) to detect formyl peptides released by bacteria and mediate chemotaxis toward bacteria (Ye et al., 2009). Binding of formyl peptides to FPRs promotes dissociation of heterotrimeric G proteins into G α i and G β \gamma, which in turn activate downstream signal transduction pathways that ultimately regulate the spatiotemporal organization of the actin cytoskeleton to drive cell migration. It is not clear, however, whether neutrophils also use the chemoattractant GPCR/Gi signaling network to promote phagocytosis of bacterial pathogens when fighting infections.

Here we show that FPRs on neutrophils detect formyl peptides derived from bacteria and mediate not only chemotaxis to chase bacteria but also phagocytosis to engulf and ingest them. We found that mouse neutrophils lacking Fpr1 and Fpr2 are defective in the phagocytosis of bacteria and the engulfment of N-formyl-Met-Leu-Phe (fMLP)-coated beads. Using a human neutrophil-like cell line, HL60, we showed that FPRs linked to Gi proteins mediate phagocytosis of

bacteria and the internalization of fMLP-coated beads. We found that chemoattractant GPCRs coupled with Gi proteins and IgG receptors linked to tyrosine kinases (Syk and Src) work independently to promote the engulfment of particles coated with either chemoattractants or opsonins. Our study reveals an evolutionarily conserved mechanism that directs neutrophils migration toward bacteria via chemotaxis and promotes their ability to engulf bacterial via “surface-dependent and opsonin-independent phagocytosis” as an essential part of innate immunity.

RESULTS

Fprs play a role in surface-associated phagocytosis of bacteria by mouse neutrophils

To examine the potential roles of chemoattractant GPCRs in the phagocytosis of bacteria, we measured the internalization of bacteria by mouse neutrophils lacking formyl peptide receptors (Fprs) (Figure 1). Fpr1 and Fpr2, which are the mouse homologues of human FPR1 and FRP2, recognize bacteria-derived chemotactic formyl peptides and guide neutrophils to chase bacterial pathogens (Liu et al., 2012). Mouse neutrophils lacking both Fpr1 and Fpr2 (Fpr1/2^{-/-}) are defective in chemotaxis toward bacteria or an fMLP source (Liu et al., 2012). We isolated neutrophils from wild-type and Fpr1/2^{-/-} mice and confirmed their genotypes by showing that fMLP stimulation triggers a transient Ca²⁺ response in wild-type but not Fpr1/2^{-/-} neutrophils (Supplemental Figure S1, A and B). Previous studies showed that isolated neutrophils do not engulf fluid-borne bacteria in suspension but internalize bacteria adhered to a surface (Colucci-Guyon et al., 2011; Lu et al., 2014). On the basis of this notion, we examined surface-associated engulfment of *Escherichia coli* by wild-type or Fpr1/2^{-/-} neutrophils. Neutrophils were first adhered to a coverslip coated with fibronectin. *Escherichia coli* labeled with pHrodo were added onto the cells. pHrodo was used to monitor bacterial engulfment and phagosome maturation. We showed that unengulfed pHrodo-*E. coli* have no fluorescence because of a high pH in the medium outside of the cells, while engulfed pHrodo-*E. coli* emitted fluorescence signals (Supplemental Figure S1C). We found that wild-type neutrophils effectively engulfed pHrodo *E. coli* (green), while Fpr1/2^{-/-} neutrophils were defective in the engulfment (Figure 1, A and B). To further quantify bacterial phagocytosis, wild-type or Fpr1/2^{-/-} neutrophils were adhered to a 96-well plate, and pHrodo-*E. coli* cells were added to the wells at 0 min. Using microscopy, we imaged pHrodo *E. coli* that emitted green fluorescence after they were engulfed, as well as neutrophils that were labeled by a cell tracker of red fluorescence at indicated time points (Figure 1C). Our quantitative analysis showed that bacterial phagocytosis by Fpr1/2^{-/-} neutrophils was significantly reduced compared with wild-type neutrophils (Figure 1D).

Fprs mediate the engulfment of fMLP-beads by mouse neutrophils

To simplify ligands on the surface of a particle, we coated latex beads with only fMLP to examine FPRs' function in phagocytosis and visualized the engulfment of fMLP-beads by wild-type and Fpr1/2^{-/-} neutrophils (Figure 1, E–H). pHrodo-fMLP-beads were added to the chambers containing adhered neutrophils, and images were recorded over a time course of 1 h (Figure 1E). Wild-type neutrophils quickly engulfed fMLP-beads (green), while Fpr1/2^{-/-} neutrophils showed a reduced ability to engulf fMLP-beads (Figure 1, E and F). Neither wild-type nor Fpr1/2^{-/-} neutrophils effectively engulfed uncoated beads (Supplemental Figure S2A). To further quantify the engulfment of fMLP coated beads, wild-type or Fpr1/2^{-/-} neutrophils were adhered to a 96-well plate, and pHrodo-fMLP

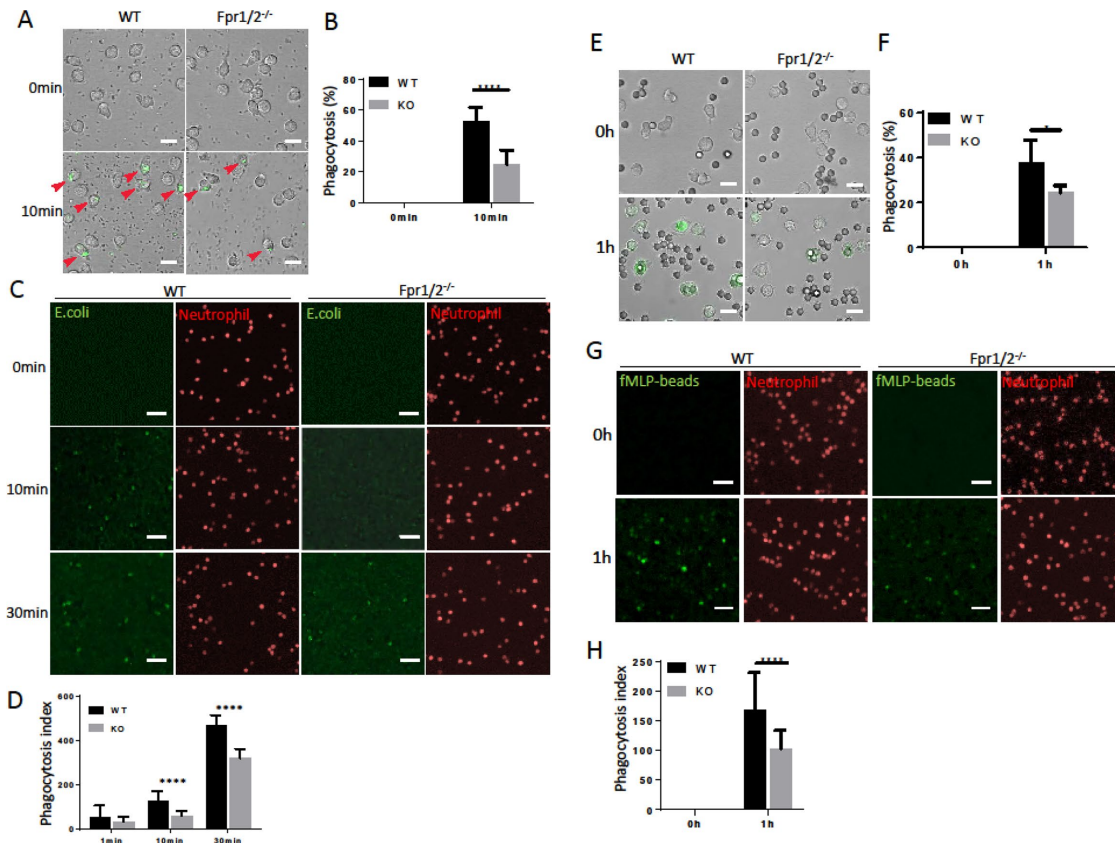


FIGURE 1: *Fpr1/2*^{-/-} mouse neutrophils are defective in phagocytosis of *E. coli* and fMLP-beads. (A) Neutrophils from wild-type and *Fpr1/2*^{-/-} mice were adhered onto fibronectin-coated coverslip. pHrodo-labeled *E. coli* were added to the cells at a 20:1 ratio at 0 min. Representative images show the engulfment of *E. coli* at 10 min using confocal microscopy. Red arrows indicate cells with engulfed pHrodo-*E. coli* (green). Scale bar, 10 μ m. (B) The cells that colocalized with green fluorescent signals and the total cells were counted from images in A. Phagocytosis percentage was calculated as the number of fluorescent cells divided by that of total cells. At least six images were taken for each condition (at least 100 cells were counted). The *p* values were calculated using Student's *t* test. *****p* < 0.001. (C) Neutrophils from wild-type and *Fpr1/2*^{-/-} mice were adhered on a fibronectin-coated 96-well plate. pHrodo-labeled *E. coli* were added to the cells at a 50:1 ratio at 0 min and incubated for the indicated time period. Cells with engulfed pHrodo-*E. coli* were imaged using the green fluorescent channel, all cells labeled with a cell tracker were imaged in the red fluorescent channel, and representative pictures are shown. Scale bar, 50 μ m. (D) Statistical analysis for C. Nine images were taken per condition. Cells were counted by Matlab (around 10,000 cells were counted), and phagocytosis rates were calculated by measuring green fluorescence intensity using MetaMorph. Phagocytosis indices were calculated as the total green intensity divided by the cell number. Mean and SD values are presented. The *p* values were calculated using paired Student's *t* test. *****p* < 0.001. (E) Neutrophils from wild-type and *Fpr1/2*^{-/-} mice were adhered onto a fibronectin-coated coverslip. pHrodo-fMLP-coated beads were added to the cells at 3:1 ratio at 0 h. Representative pictures show the engulfment of fMLP-beads at 1 h using a confocal microscope. Scale bar, 10 μ m. (F) Number of cells that colocalized with green fluorescent signals and that of the total cells were counted from images in E. Phagocytosis percentages were calculated as the number of fluorescent cells divided by the number of total cells. At least six images were taken for each condition. The *p* values were calculated using Student's *t* test. **p* < 0.05. (G) Neutrophils from wild-type and *Fpr1/2*^{-/-} mice were adhered on fibronectin-coated 96-well plates, and pHrodo-fMLP-coated beads were added to the cells at a 3:1 ratio at 0 h. Representative images show engulfed fMLP-beads in the green fluorescent channel and neutrophils in the red fluorescent channel. Scale bar, 50 μ m. (H) Statistical analysis for G. Cell number and green fluorescence intensity were measured as in D. Phagocytosis indices were calculated as the total green intensity divided by the number of cells. Mean and SD values are presented. The *p* values were calculated using paired Student's *t* test. *****p* < 0.001.

beads were added to the wells. Using fluorescence imaging, we counted engulfed pHrodo-fMLP-beads that emitted green fluorescence (green) and neutrophils that were labeled by the cell tracker (red) at 1 h (Figure 1G). Our quantitative analysis showed that the *Fpr1/2*^{-/-} neutrophils have less ability to engulf fMLP-beads than wild-type neutrophils (Figure 1H). Together, our results suggest that fMLP-coated beads activate Fprs to promote the engulfment of the beads.

Both IgG- and fMLP-coated beads induce the engulfment of the beads by HL60 cells

To explore the role of chemoattractant GPCR-mediated *G_i* signaling in phagocytosis by human neutrophils, we examined the internalization of latex beads by HL60 cells (Gallagher *et al.*, 1979). HL60 cells express FPRs to mediate migration toward bacteria, and they also express IgG receptors, such as Fc γ receptors that are coupled with tyrosine kinases, to mediate phagocytosis of

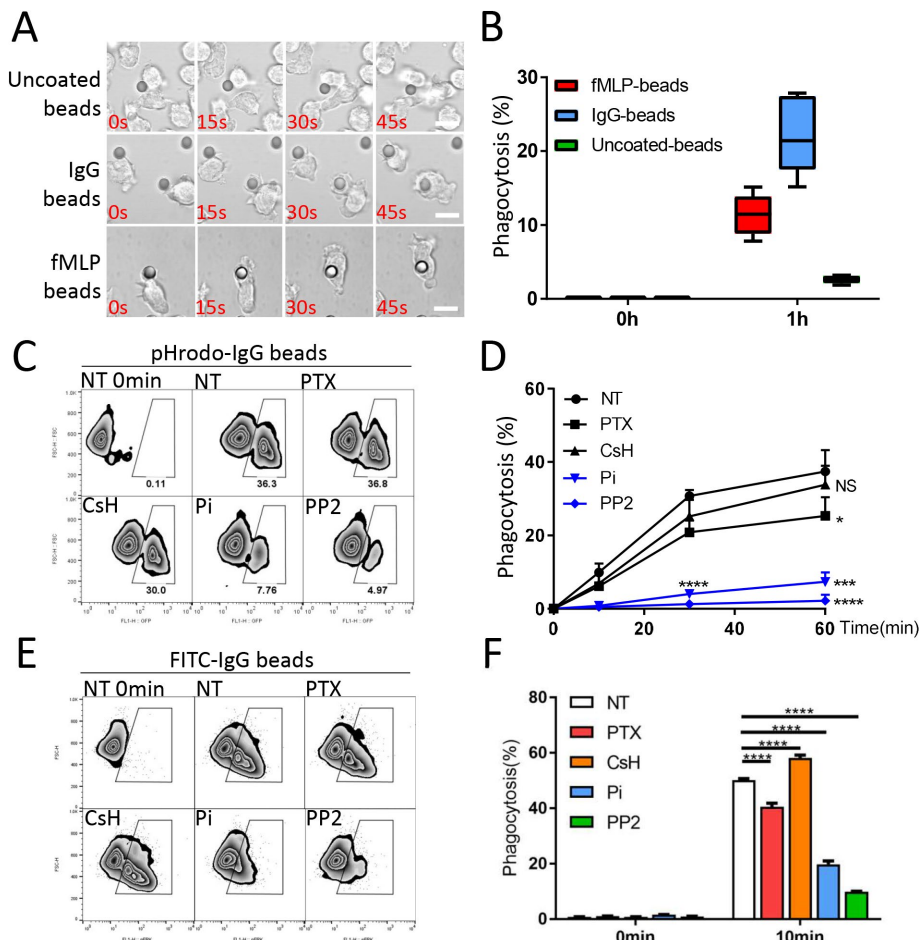


FIGURE 2: Engulfment of IgG-beads is mediated by tyrosine kinases but not a GPCR/Gi pathway. (A) HL60 cells were adhered onto fibronectin-coated cover slips. Uncoated beads, IgG-beads, and fMLP-beads were added to cells. Images showing cell-bead interactions were taken using a confocal microscope. At least three time-lapse movies were acquired for each type of bead. Scale bar, 5 μ m. (B) HL60 cells were adhered onto fibronectin-coated 96-well plates. pHrodo-labeled fMLP-beads, IgG-beads, and uncoated beads were added to cells at 0 h. Nine images were acquired for each condition. Phagocytosis percentage was calculated as the number of fluorescent cells divided by the number of total cells. (C) HL60 cells were either untreated or treated with PTX, CsH, Pi, or PP2. Cells were starved in suspension, and pHrodo-labeled IgG-coated beads were added to cells. The mixture was incubated in 37°C for indicated time period. Fluorescent cells were detected by flow cytometry. Representative pictures of flow cytometry analyses were shown at 0 min for no treatment (NT) and 60 min for all treatment. (D) Statistical analysis for experiments shown in C. In each sample, 10⁵ cells were analyzed. Experiments were repeated three times. The *p* values were calculated using Student's *t* test. *****p* < 0.001, ****p* < 0.005, **p* < 0.05, NS: not significant. (E) HL60 cells were treated as in Figure 1C, and FITC-IgG-coated beads were added to the cells. The mixture was incubated in 37°C for indicated time period, and fluorescent signals outside of cells were quenched before flow cytometry analysis. Representative graphs show data obtained at 0 min for no treatment (NT) and 10 min for all samples. (F) Statistical analysis for experiments shown in E. In each sample, 10⁵ cells were analyzed. Experiments were repeated three times. The *p* values were calculated using Student's *t* test. *****p* < 0.001, NS: not significant.

opsonized pathogens (Bestebroer *et al.*, 2010; Underhill and Goodridge, 2012). To examine whether immobilized chemoattractants on the surface of a particle are sufficient to promote particle engulfment by human neutrophils, we visualized the engulfment of beads coated with different ligands using live-cell imaging (Figure 2A). Beads without any ligand (uncoated beads) were found to make contacts with cells but not engulfed by the cells. In contrast, beads coated with IgG (IgG-beads) were quickly internalized after making contact with the cells, confirming

that binding of IgG to IgG receptors (FcγRs) induces internalization of IgG-beads (Aderem and Underhill, 1999). fMLP-beads were also quickly engulfed by HL60 cells following the interaction between the beads and the cells (Figure 2A). Quantitative analysis showed that the cells effectively internalized both IgG-beads and fMLP-beads but not uncoated beads (Figure 2B). Our results suggest that chemoattractants immobilized on the surface of a particle act like IgG opsonins to promote the engulfment of particles.

Activation of tyrosine kinases is required for the engulfment of IgG-coated beads

Several studies have shown that an opsonized particle binding to receptors that activate tyrosine kinases, including Src and Syk, leads to the engulfment of an opsonized particle (Hishikawa *et al.*, 1991; Berton *et al.*, 2005; Nunes and Demareux, 2010). To confirm the role of Src and Syk kinases in the engulfment of opsonized particles, we treated HL60 cells with C₁₅H₁₆CIN₅ (PP2) or Pi (Piceatannol) to block phosphorylation (activation) of Src family and Syk, respectively (Hanke *et al.*, 1996; Sada *et al.*, 2001) and measured the engulfment of IgG-beads using flow cytometry. IgG-beads labeled with pHrodo were used for monitoring the process of engulfment and phagosome maturation (Figure 2, C and D), and IgG-beads labeled with fluorescein isothiocyanate (FITC) were used to show the engulfment process (Figure 2, E and F). Before the cytometry analysis of the engulfment of FITC-IgG beads, trypan blue was added to quench fluorescence from FITC-labeled beads outside of cells (Bjerknes and Bassøe, 1984). Cells with fluorescence signal are those with internalized pHrodo-IgG beads in phagolysosome (Figure 2, C and D) or engulfed FITC-IgG beads (Figure 2, E and F). When treated with PP2 or Pi, the cells could no longer effectively engulf pHrodo-IgG beads or FITC-IgG beads. However, when treated with pertussis toxin (PTX) or Cyclosporin H (CsH), two drugs blocking chemoattractant GPCR/Gi signaling, the cells still retained the ability to engulf IgG-beads (Figure 2, D and F). PTX is a bacteria produced protein, composed of an A-promoter and a B-oligomer, and the A-promoter exerts ADP-ribosyltransferase activity on the Gαi proteins, thereby inhibiting the coupling between GPCR and G protein (Gao *et al.*, 1999; Hartt *et al.*, 1999; Mangmool and Kurose, 2011). However, CsH selectively inhibits the binding of formyl peptides to FPRs (Wenzel-Seifert and Seifert, 1993; Stenfeldt *et al.*, 2007). Thus, our results demonstrate that IgG receptor/tyrosine kinase signaling works independently of chemoattractant GPCR/Gi signaling to promote the engulfment of IgG-beads.

The engulfment of fMLP-beads is mediated by the chemoattractant GPCR/Gi and independent of IgG receptor/tyrosine kinase signaling

To further explore the functions of chemoattractant GPCR/Gi signaling in phagocytosis by HL60 cells, we investigated the effects of drugs that block either GPCR/Gi signaling or tyrosine kinases in the engulfment of fMLP-beads. We first examined specificity of the drugs by measuring their effects on chemoattractant GPCR/Gi-mediated neutrophil chemotaxis. When the cells were treated with CsH or PTX, fMLP stimulation could no longer induce any Ca^{2+} response, and the cells failed to undergo chemotaxis toward an fMLP source (Supplemental Figure S3, A and B). However, treatment with PP2 neither significantly affected fMLP-mediated Ca^{2+} flux nor eliminated cell chemotaxis toward the fMLP source, while the treatment with Pi partially inhibited chemotaxis, consistent with previous reports that Pi blocks PI3K signaling and reduces cell adhesion, thereby causing defects in chemotaxis (Kwon *et al.*, 2012). Thus, our results confirmed that CsH or PTX effectively blocks FPR-mediated signaling and chemotaxis.

We subsequently measured surface-associated engulfment of fMLP-beads by HL60 cells treated with these drugs (Figure 3). pHrodo-fMLP-beads (Figure 3A) or FITC-fMLP-beads (Figure 3C) were added to the adhered cells. fMLP-beads, like IgG-beads, were internalized by the cells without drug treatment (Figure 3, A and C, NT). After treatment with PTX or CsH, the cells lost the ability of engulfing pHrodo-fMLP-beads (Figure 3, A and C) or FITC-fMLP-beads (Figure 3, B and D). After treatment with Pi, the cells failed to engulf both pHrodo-fMLP-beads and FITC-fMLP-beads, consistent with the notion that Pi inhibits PI3K and cell adhesion, thereby causing defects in the engulfment of fMLP-beads (Kwon *et al.*, 2012). After the cells were treated with PP2, we detected the internalization of FITC-fMLP-beads (Figure 3, B and D) but not pHrodo-fMLP-beads (Figure 3, A and C), suggesting that blocking Src kinases did not eliminate the engulfment of fMLP-beads but might have inhibited the formation of phagolysosome with a low-pH environment (Li *et al.*, 2016). We also examined surface-associated engulfment of IgG-beads by HL60 cells (Figure 3, E and F). Consistent with the results obtained from cells in suspension, adhered neutrophils effectively engulfed pHrodo-IgG beads and FITC-IgG beads; however, after treatment of Pi or PP2, the cells lost their ability to internalize either IgG-beads. In contrast, the cells were

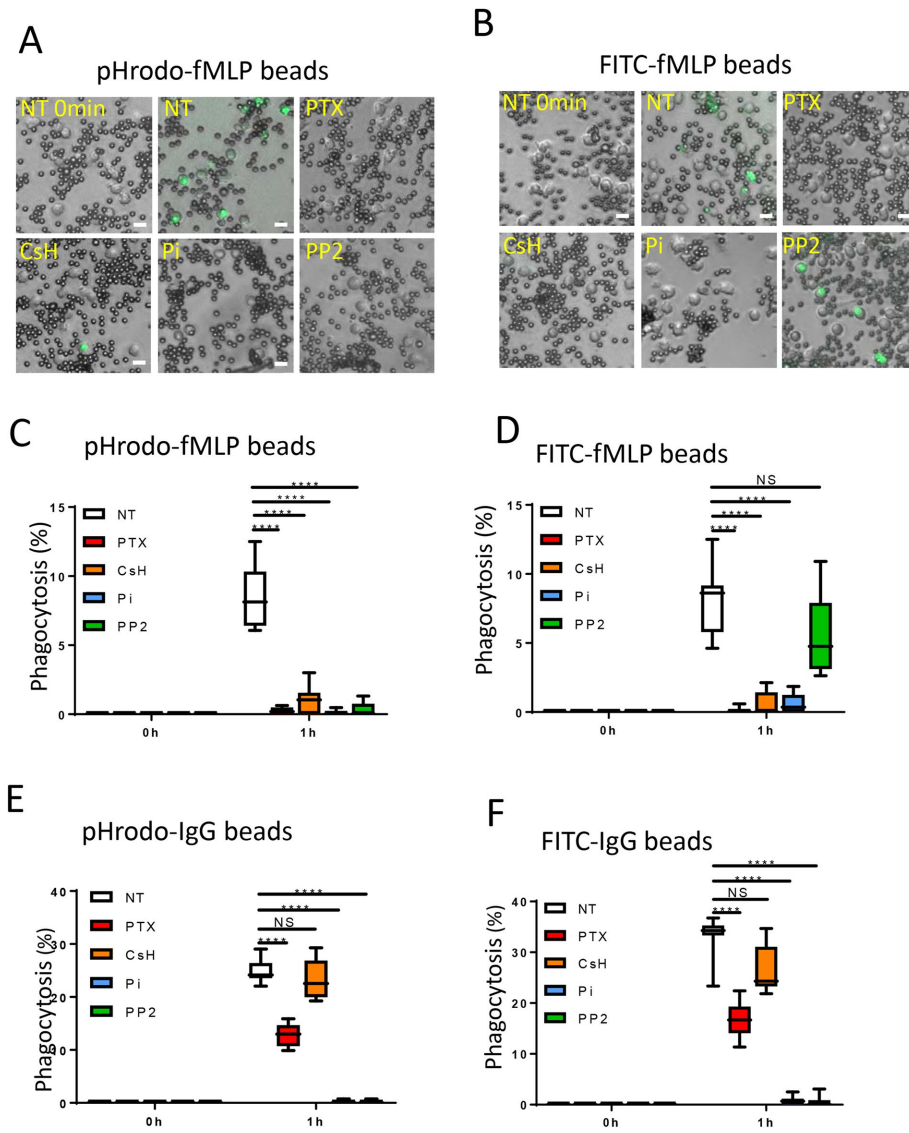


FIGURE 3: Engulfment of fMLP-beads is mediated by GPCR/Gi pathway but not tyrosine kinases. (A) HL60 cells were either untreated or treated with PTX, CsH, Pi, or PP2. They were starved in fibronectin-coated 96-well plate for 1.5 h, and then pHrodo-fMLP-coated beads were added to cells at time 0 and incubated for 1 h. Representative pictures show merged images of bright field (showing cells and beads) and the green channel (showing phagocytosed fMLP beads) at time 0 for the NT (no treatment) sample and 1 h for all samples. Scale bar, 10 μ m. (B) HL60 cells were treated as in A. FITC-labeled fMLP-coated beads were added to cells at time 0 and incubated for 1 h before signal quenching with trypan blue. Representative pictures show merged images of bright field and green channel. Green fluorescence indicates engulfed fMLP beads. Scale bar, 10 μ m. (C) Statistical analysis for A. Phagocytosis percentage was calculated as the number of fluorescent cells divided by the number of total cells from nine images acquired for each condition. The *p* values were calculated using Student's *t* test. *****p* < 0.001. (D) Statistical analysis for B. Phagocytosis percentage was calculated as the number of fluorescent cells divided by the number of total cells from nine images acquired for each condition. The *p* values were calculated using Student's *t* test. *****p* < 0.001, NS: not significant. (E) HL60 cells were either untreated or treated with PTX, CsH, Pi, or PP2 and were starved in fibronectin-coated 96-well plate for 1.5 h, and then pHrodo-IgG-beads were added to cells at time 0 and incubated for 1 h. Green fluorescence indicates engulfed IgG-beads. Phagocytosis percentage was calculated as the number of fluorescent cells divided by the number of total cells from nine images acquired for each condition. The *p* values were calculated using Student's *t* test. *****p* < 0.001, NS: not significant. (F) HL60 cells were treated as in E. FITC-IgG beads were added to cells at time 0 and incubated for 1 h before signal quenching with trypan blue. Phagocytosis percentage was calculated as the number of fluorescent cells divided by the number of total cells from nine images acquired for each condition. The *p* values were calculated using Student's *t* test. *****p* < 0.001, NS: not significant.

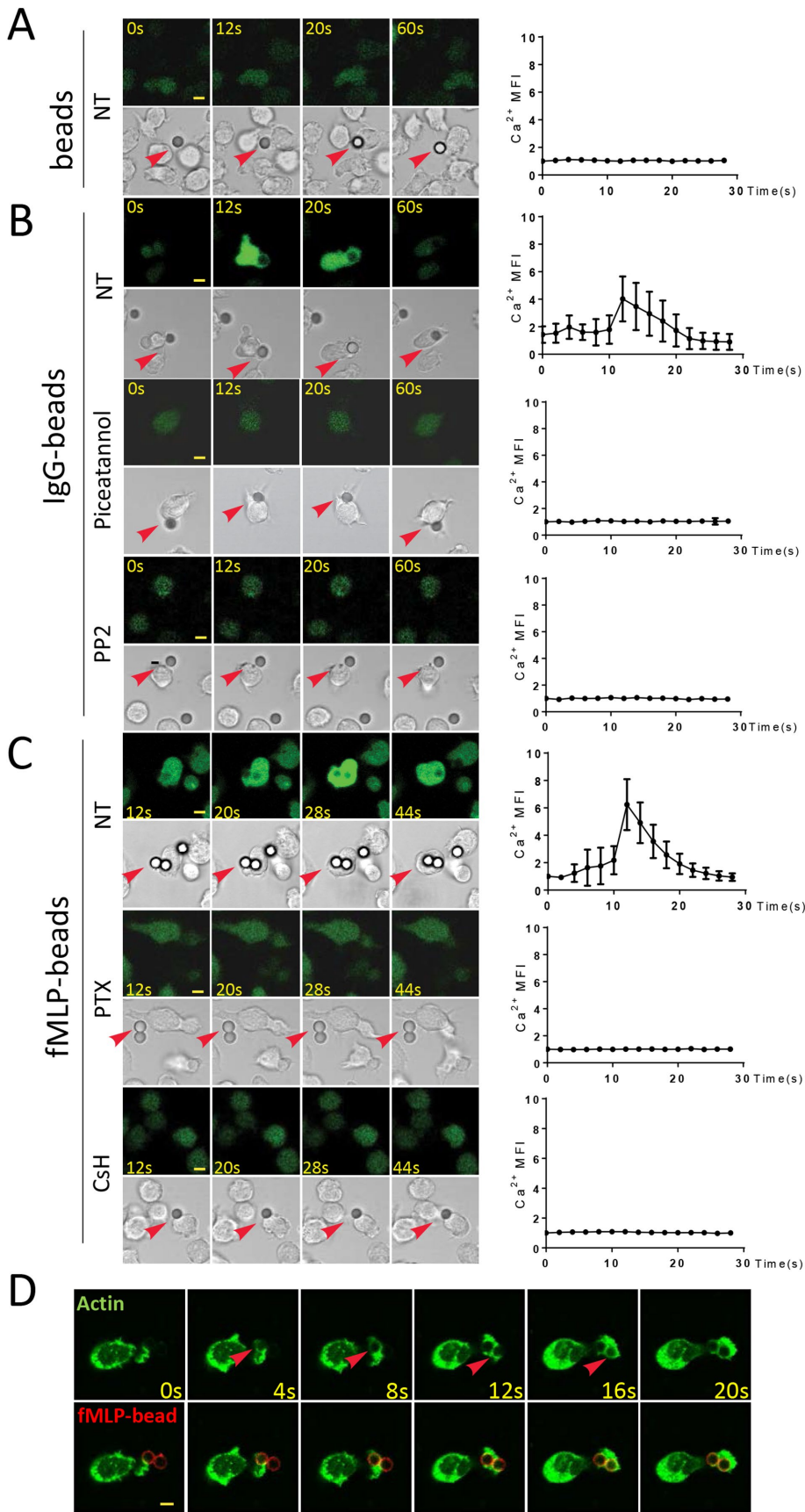


FIGURE 4: fMLP-beads induce calcium flux and actin polymerization. (A) HL60 cells were stained with Fluo-4, placed on fibronectin-coated coverslip and monitored under a microscope. Noncoated beads were added to cells, and images were taken with both bright-field and green fluorescent

still able to engulf the beads after treatment of PTX or CsH (Figure 3, E and F). Our results suggest that neutrophils, when properly adhered to the surface, utilize the chemoattractant GPCR/Gi signaling pathway, independent of receptor/tyrosine kinase signaling, to promote the engulfment of fMLP-beads.

fMLP-beads induce chemotactic responses and formation of phagocytic cups

To monitor receptor-mediated signaling and the engulfment simultaneously, we imaged the Ca^{2+} response and the engulfment process triggered by ligand-coated beads (Figure 4). Previous studies showed that binding of an opsonized particle to IgG receptors activates tyrosine kinases Src and Syk, which subsequently triggers Ca^{2+} influx and the engulfment of the particle (Hishikawa *et al.*, 1991; Berton *et al.*, 2005; Nunes and Demareux, 2010). Beads were added to a chamber containing HL60 cells that were labeled with Fluo-4, a fluorescent calcium indicator (Jiao *et al.*, 2005). Uncoated beads could trigger neither Ca^{2+} responses nor the engulfment of the beads (Figure 4A), while IgG-beads triggered Ca^{2+} influx and the engulfment of the beads (Figure 4B), indicating that binding of IgG-beads to Fc γ R receptors induced Ca^{2+} influx during the engulfment process. Cells that were treated with either PP2 or Pi failed to trigger either Ca^{2+} influx or engulfment of the beads (Figure 4B), confirming the notion that blocking the function of Src or Syk

channels. Left panel shows representative images for bead–cell interactions. Red arrows indicate the beads which interact with the cells. Scale bar, 5 μm . In the right panel, Fluo-4 intensity indicating intracellular calcium flux was quantified using ImageJ and analyzed using Prism. More than three time-lapse sequences were obtained. (B) Cells were either untreated or treated with Piceatannol or PP2 and stained with Fluo-4. IgG-beads were then added to the cells. Images were taken and analyzed as in A. (C) Cells were either untreated or treated with PTX or CsH and stained with fluo-4. fMLP-beads were then added to the cells. Images were taken and analyzed as in A. (D) HL60 cells stably expressing actin-mCherry were used to monitor actin dynamics. fMLP/Alexa488-coated beads were added to cells on cover slips, and the engulfment process was recorded microscopically. Red arrows indicate the formation of phagocytic cup. Green, actin; red, beads. Scale bar, 5 μm . More than three time-lapse sequences were acquired.

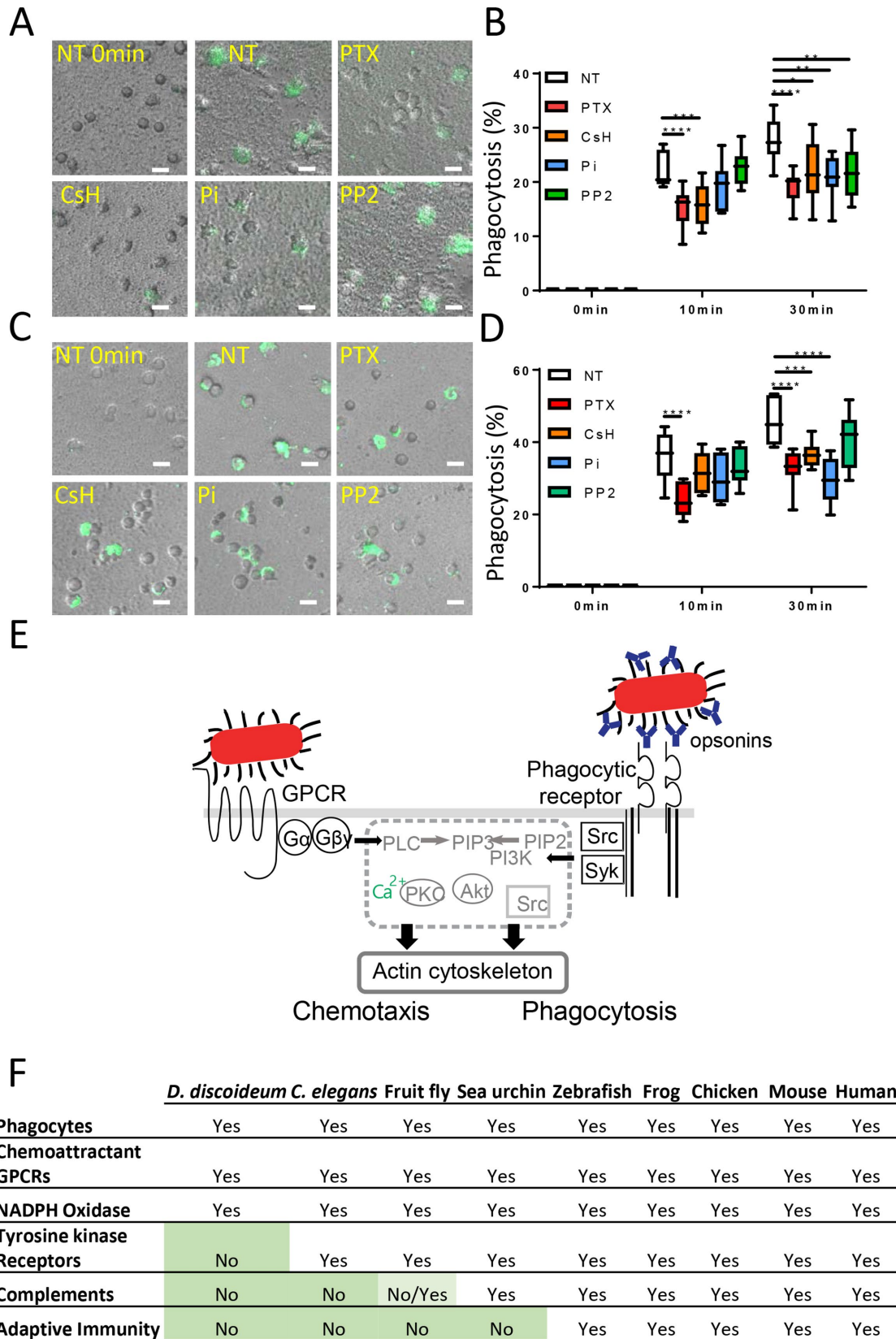


FIGURE 5: Both GPCR/Gi signaling and phagocytic receptor/tyrosine kinase signaling play roles in bacterial phagocytosis. (A) HL60 cells were either untreated or treated with PTX, CsH, Pi, or PP2 and were placed in a fibronectin-coated 96-well plate. pHrodo-*E. coli* were added to cells at 0 min and incubated for 10 or 30 min. Representative merged images of bright field and the green channel are shown. Green fluorescence indicates phagocytosed *E. coli*. Scale bar, 10 μ m. (B) Statistical analysis for A. Phagocytosis percentage was calculated as the number of fluorescent cells divided by the number of total cells from nine images acquired for each condition. **** $p < 0.001$, *** $p < 0.005$,

inhibits both IgG receptor (IgG/FcγR)-induced Ca²⁺ response and particle engulfment. We also observed that fMLP-beads induced a transient Ca²⁺ flux and the engulfment of the fMLP-beads (Figure 4C). When the cells were treated with PTX or CsH to inhibit Gi signaling or the activation of FPRs, respectively, fMLP-beads triggered neither a Ca²⁺ response nor the engulfment of the beads, suggesting that activation of FPRs and Gi signaling mediates fMLP-bead-induced Ca²⁺ flux and the engulfment of fMLP-beads.

To examine whether a chemoattractant-coated bead can induce the formation of a phagocytic cup, we imaged the actin cytoskeleton in a live cell during engulfment of an fMLP-bead (Figure 4D). Fluorescence-labeled fMLP-beads labeled by Alexa 488 (pseudocolored red) were added to a chamber containing cells expressing actin-mCherry (pseudocolored green) (Figure 4D and Supplemental Figure S4A). We found that binding of an fMLP-bead to the cell surface induced actin polymerization surrounding the bead to form a phagocytic cup (4 s and 12 s, arrows), followed by the engulfment of the bead. Together, our results suggest that fMLP immobilized on the surface of a particle activates chemoattractant GPCR/Gi signaling to induce chemotactic responses, including Ca²⁺ mobilization and actin polymerization, which leads to phagocytic cup formation and subsequent particle engulfment. Because fMLP-induced Ca²⁺ flux and the formation of phagocytic cup occurred immediately after cells contact with the beads, we suggest that FPR-induced Gi signaling, instead of the priming effect from FPR signaling, plays a critical role in the engulfment of fMLP-beads.

Both GPCR/Gi signaling and IgG receptor/tyrosine kinase signaling play roles in bacterial phagocytosis

To further explore the role of chemoattractant GPCRs and IgG receptors in phagocytosis of bacteria by human neutrophils, we quantified the internalization of bacteria by HL60 cells treated with various drugs that block signaling of either chemoattractant GPCR/Gi or IgG receptors. Adhered HL60 cells were added with pHrodo-labeled *E. coli* (Figure 5, A and B) or FITC-labeled *E. coli* (Figure 5, C and D), and images were taken at different time points. Cells treated with drugs, which inhibit either chemoattractant GPCR/Gi signaling (PTX and CsH) or tyrosine kinases (Pi and PP2), displayed a reduced ability to uptake bacteria. Furthermore, when both GPCR/Gi signaling and tyrosine kinases were inhibited by the drug treatment, cells displayed an even greater diminution of bacterial engulfment (Supplemental Figure S5), suggesting that blocking both GPCR and tyrosine pathways causes a synergistic inhibitory effect. Taken together, our results support the notion that both chemoattractant GPCRs/Gi signaling and tyrosine kinases signaling contribute to bacterial phagocytosis in the absence of opsonins (Figure 5E). It is also likely that the engulfment is further promoted by some scavenger receptors binding to *E. coli* (Canton et al., 2013).

DISCUSSION

Our study indicates that neutrophils use a chemoattractant GPCR-mediated engulfment mechanism to eliminate bacteria via surface-

associated phagocytosis in the absence of opsonins. This notion challenges the dogma in the field of immunology that human phagocytes, including neutrophils and macrophages, can effectively ingest bacteria only when they were coated with specific opsonins, such as complements or IgGs (Underhill and Ozinsky, 2002; Bestebroer et al., 2010; Rougerie et al., 2013). Over the years, phagocytic receptors, including FcγR for IgGs and complement receptors, and their associated tyrosine kinases have been identified for binding the opsonized microbe and inducing actin polymerization for the formation of phagocytic cups for microbial engulfment (Bestebroer et al., 2010; Freeman and Grinstein, 2014b). However, several previous studies did suggest that neutrophils engulf bacteria without opsonins. For example, Wood et al. (1946a,b) reported that neutrophils in rat lungs directly attack and ultimately destroy pneumococci via surface-mediated phagocytosis without the aid of an intermediary opsonin. In addition, a study in zebrafish showed that neutrophils, unlike macrophages, barely engulf bacteria in the blood or fluid-filled body cavities as an innate immune response, but they efficiently sweep up bacteria that are unopsonized but surface associated (Colucci-Guyon et al., 2011). A recent study also showed that adherent human neutrophils efficiently engulf and kill *Staphylococcus aureus* without any opsonins although they cannot effectively engulf these bacteria without the addition of opsonins in suspension (Lu et al., 2014). These findings suggest that when floating in a fluid medium, neutrophils rely on opsonins to bind and catch bacteria for phagocytosis, but when associated with suitable surfaces, neutrophils effectively catch and kill bacteria via phagocytosis in the absence of opsonins. It is well known that neutrophils migrate only on certain surfaces, such as glass coated with fibronectin (Millius and Weiner, 2009). Our study indicates that when attached to a suitable surface, neutrophils use the chemoattractant GPCR/Gi signaling machinery to mediate actin polymerization for both directional cell migration and the engulfment of particles coated with chemoattractants.

Phagocytes use the chemoattractant GPCR/G-protein machinery or the receptor/tyrosine kinase machinery to control actin polymerization for catching and engulfing bacteria (Figure 5E). Phagocytosis can be observed in amoeboid cells from many eukaryotic organisms, such as *D. discoideum*, *Caenorhabditis elegans*, fruit fly, sea urchin, zebrafish, frog, chicken, mouse, and human (Beck and Habicht, 1996; Cosson and Soldati, 2008; Ricklin et al., 2016; Underhill et al., 2016). The central components of the phagocytic machinery found in these organisms are summarized in Figure 5F. The comparative analysis of these components shed light on the evolutionary origins of some fundamental features of human innate immunity. The primitive phagocytes of *D. discoideum* do not encode tyrosine kinases, and they use chemoattractant GPCR fAR1 to mediate actin polymerization for not only chemotaxis to catch bacteria but also phagocytosis to eat bacteria (Pan et al., 2016). In addition, *D. discoideum* contains members of Nox-family NADPH oxidase that produce superoxide ions and acidification of phagolysosome to kill internalized bacteria

p* < 0.01, **p* < 0.05. (C) HL60 cells were treated as in A. FITC-*E. coli* were added to cells at 0 min and incubated for 10 or 30 min before signal quenching with trypan blue. Representative merged images of bright field and the green channel are shown. Green fluorescence indicates phagocytosed *E. coli*. Scale bar, 10 μm. (D) Statistical analysis for C. Phagocytosis percentage was calculated as the number of fluorescent cells divided by the number of total cells from nine images acquired for each condition. **p* < 0.001, ****p* < 0.005. (E) GPCR-mediated bacterial phagocytosis requires G-protein machinery, while phagocytic receptor-mediated phagocytosis requires activation of Src and Syk kinases. They both lead to actin-dependent phagocytosis. (F) Summary of different components required for phagocytosis in phagocytes from simple organisms to human.

(Sumimoto, 2008). *Caenorhabditis elegans* and fruit fly encode tyrosine kinases that have the potential to associate with scavenger receptors for phagocytosis (Stuart and Ezekowitz, 2008). The lower eukaryotic organisms, such as *D. discoideum* and *C. elegans*, encode neither a complement system nor an adaptive immune system (Beck and Habicht, 1996; DeVries *et al.*, 2006; Cosson and Soldati, 2008). Animals ranging from sea urchin to human have a version of the complement system, and vertebrates including human have both a complement system and an adaptive immunity (antibody-based immune system). It appears that a complement system was added in sea urchin and retained in animals with fluid-filled body cavity or a circulatory system, and an adaptive immunity was then acquired as the latest feature by the vertebrate immune system. Since phagocytes from all organisms have chemoattractant GPCR/G-protein machinery, we propose that chemoattractant GPCR-mediated surface-associated phagocytosis by neutrophils is an ancient and evolutionarily conserved mechanism of the innate immunity for fighting against invading bacteria.

How the FPR/Gi signaling machinery detects ligands on the surface of bacteria to promote phagocytosis is not clear. We showed that binding of fMLP beads to FPRs activates Gi-signaling, which leads to an actin-dependent engulfment of the beads independent of Src/Syk activation. However, our results do not determine whether FPRs facilitate binding of bacteria, internalization of bacteria or both steps. We cannot exclude the possibility that FPRs promote binding of bacteria but other receptor signaling pathways drive the ingestion of bacteria. Formal peptide receptors from mammalian species, including human and mouse, detect various N-terminal formyl signal peptides at nanomolar range. FPRs employ an unusual detection mechanism that combines structural promiscuity with high specificity and sensitivity, thereby detecting over thousands of predicted bacterial signal peptides yet maintaining selectivity (Bufe and Zufall, 2016). There are a few major outer membrane proteins (lipoproteins, TolG proteins, and matrix proteins), which exist in very large quantities on bacteria surfaces with N-formyl signaling peptides (Sjostrom *et al.*, 1987). Bacteria continuously secrete formyl proteins to the cell membrane and cleave them to release formyl signal peptides. It is possible that formyl peptides exist on the surface of bacteria and serve as ligands for FPR-mediated engulfment. It is likely that phagocytes can take up bacteria or beads without specific receptors, including IgG receptors or FPRs, by using another mechanism, such as micropinocytosis. However, the engulfment of particles via micropinocytosis is not efficient. It is also possible that formyl peptides released from bacteria activate FPR/Gi signaling, which subsequently promotes the formation of macropinosomes for bacterial engulfment (Swanson, 2008). Future studies are needed to further dissect detailed mechanisms underlying the FPR/Gi-mediated bacterial engulfment.

MATERIALS AND METHODS

Cell culture and stable cell line establishment

The HL60 cell line stably expressing CXCR2 (HL-60-CXCR2) was a gift from Ann Richmond at Vanderbilt University. Cells were cultured in 1640 RPMI medium with 25 mM HEPES (Quality Biological), 20% fetal bovine serum (FBS), and 1% penicillin streptomycin (all from Life Technologies unless mentioned) at 37°C with 5% CO₂. To differentiate cells, dimethyl sulfoxide was added to culture medium at a final concentration of 1.3%, and cells were incubated for 5 d.

HL60-CXCR2 cells were infected by the lentivirus encoding human actin-mCherry gene (Vectalys, France). Briefly, 100 μ l viral particles and 5 μ g/ml Polybrene were added to 10⁶ cells and selected

by puromycin (R&D Systems). Cells were transferred to fresh medium the next morning and incubated for 48 h before subculturing with the addition of puromycin. After three to four passages, cells were ready for differentiation.

Purification of mouse neutrophils

C57/B6 wild-type and Fpr1/2 double mutant (Fpr1^{-/-} and Fpr2^{-/-}) mice were from Ji Ming Wang's lab, National Cancer Institute, National Institutes of Health (NIH). Bone marrow was collected from the hind legs. Briefly, one end of the bone was cut open, and bone marrow was collected by centrifugation at 8600 \times g for 10 s. Red blood cells were removed with ammonium-chloride-potassium buffer (Lonza) at room temperature. After the cells were counted, cells were subject to neutrophil isolation using a mouse neutrophil isolation kit (Miltenyi Biotec; order no. 130097658). Collected neutrophils were stored in PBS supplemented with 2% FBS and 2 mM EDTA at 4°C. The purity of neutrophils was determined by staining the cells with mouse Gr-1/Ly-6G PE-conjugated antibody and CD11b FITC-conjugated antibody (R&D Systems). The purity was above 95% (unpublished data).

Preparation of beads

Biotin was linked to the side chain of lysine at the C-terminus of fMLP. IgG-biotin was purchased from Jackson ImmunoResearch (cat. no. 009-060-003). FITC-biotin was purchased from Thermo Fisher (cat. no. 22030). Streptavidin-coated microspheres of 5 μ m diameter were purchased from Bangs Laboratories, India (cat. no. CP01N). Beads were freshly prepared by incubating the corresponding ligand with beads for 1 h at room temperature in HBSS buffer and washed twice before use. IgG-coated or uncoated beads were stained with FITC-anti-human IgG Fc antibody (Biolegend, #409309) for 30 min on ice. The coating efficiencies were examined by flow cytometry analysis after a wash, and data were processed using FlowJo. IgG coating showed near 100% efficiency (unpublished data).

Confocal microscopy

LabTekII #1.5 one- or eight-chambered slides (Nalge Nunc) were coated with 100 μ g/ml Fibronectin (Sigma) for 1 h at room temperature before the cells were seeded in starving medium. Mouse neutrophils were not treated, and HL60 cells were untreated or treated with drugs for 4 h (1 μ M pertussis toxin; Life Technologies, Cat. no. PHZ1174), 30 min (50 μ M Piceatannol; Sigma Aldrich Cat. no. P0453, or 30 μ M PP2 Cat. no. P0042), or 5 min (10 μ M Cyclosporin H; Enzo Life Sciences, Cat. no. ALX-380-286-M005), respectively. After 1.5 h starvation, HL60 cells were ready for confocal microscopy. LSM780 40 \times /N.A. 1.4 lens or LSM880 40 \times /N.A. 1.4 lens (Carl Zeiss) was used for the experiments, and a 37°C environment chamber was applied throughout the experiments. For phagocytosis visualization, pHrodo-*E. coli* was added to cells at a 20:1 ratio; further, pHrodo-beads were added to the cells at a 3:1 ratio. At least six images were acquired at each time point, and at least 300 cells were counted. The cells that colocalized with the fluorescent signal and total cells for each picture were counted. Percentage of phagocytosis was calculated by dividing the number of fluorescent cells by that of total cells in each picture. Statistical analysis was done using Prism software. For recording phagocytosis, time-lapse sequences of 8 min were taken at 2.5- to 3-s intervals.

To monitor calcium response, cells were stained with 1 μ M Fluo-4 (Life technologies) for 30 min and washed before being seeded to the chambered slides. Beads were added to the slides and cell response was recorded by time-lapse microscopy. Fluorescence intensity was analyzed using Zen2012 (Carl Zeiss), ImageJ (NIH), and Prism.

To monitor phagocytic cup formation, HL60 cells were starved in fibronectin-coated cover slips for 1.5 h and placed on LSM880 Airyscan with 40×/N.A. 1.4 lens. Then beads were added to the cells, and pictures were taken at 4-s intervals with Z-stack to record actin polymerization. Live-cell imaging experiments were repeated at least three times, and data were analyzed using Zen2012 and ImageJ.

Ninety-six-well phagocytosis assay

pHrodo-fMLP-beads and pHrodo-IgG-beads were made by incubating fMLP-biotin/IgG-biotin and pHrodo Green STP ester (Life Technologies; cat. no. P35369) with beads for 1 h at room temperature and washed twice. HL60 cells were starved for 1.5 h, and the drugs were added for 4 h (1 μM pertussis toxin), 30 min (50 μM Piceatannol or 30 μM PP2) or 5 min (10 μM Cyclosporin H), respectively. pHrodo Green *E. coli* Bioparticles Conjugate (Life Technologies; cat. no. P35366) was sonicated for 5 min before use.

For surface phagocytosis assays using mouse neutrophils, 96-well black-wall clear-bottom plates were coated with 100 μg/ml fibronectin for 1 h at 37°C. Purified neutrophils (8×10^4 cells/well) were stained with Cell tracker orange (Thermo Fisher) for 20 min at 4°C and were then attached to the wells for 15 min at room temperature. For assays using HL60 cells, cells were seeded to 96-well plates and starved for 1.5 h at 37°C before experiments. pHrodo-*E. coli*, FITC-*E. coli* bioparticles or pHrodo-labeled beads, FITC-labeled beads were added to the cells at a ratio of 50:1 (*E. coli* vs. cells) or 3:1 (beads vs. cells). The plates were centrifuged at $500 \times g$ for 5 min at 4°C and then incubated at 37°C for the indicated time. Phagocytosis was stopped by incubating the plates at 4°C for 15 min. To visualize and count cells, an EVOS (Life Technology) microscope was used. Images were taken using the green channel and the orange channel for the same view with mouse neutrophils using 10× lens (around 1000 cells per picture). Or green-channel and bright-field pictures were taken for HL60 cells using a 20× lens (around 300 cells per picture). Three views were taken in each well, and three wells were examined in each condition. Image data were analyzed using MetaMorph and Matlab. For mouse neutrophils and HL60 cells, the data represent the fluorescent cell number/total cell number in each image. The *p* values were calculated using Student's *t* test.

Flow cytometry

Starved HL60 cells were spun down and resuspended at a density of 2×10^7 cells/ml. pHrodo-IgG-beads were added to cells at a ratio of 3:1 and incubated at 37°C for 10 min or 30 min. FITC-IgG-beads were added to cells and incubated for 10 min before trypan blue quenching. The reaction was stopped by adding the ice-cold fluorescence-activated cell sorting buffer and subjecting to flow cytometry analysis. Cells (10^5) were recorded for each sample with three replications, and experiments were repeated three times. Data were analyzed using FlowJo and Prism.

EZ-TAXIScan assay

The EZ-TAXIScan chamber (Effector Cell Institute, Japan) was used to monitor chemotaxis of cells. The apparatus was assembled according to manufacturer's instructions. Cover glass was coated with 1% bovine serum albumin (BSA) in starving medium for 1 h at room temperature. Cells were resuspended in 0.1% BSA medium, and 50 nM fMLP was added to establish a gradient for chemotaxis. Cell migration was recorded for 30 min at 15-s intervals, and the data were analyzed using DIAS software and ImageJ.

ACKNOWLEDGMENTS

We thank Susan Pierce, Polly Matzinger, Dustin Parsons, and Xin Xiang for reading the manuscript and providing helpful suggestions; Ann Richmond for the gift of the HL60-CXCR2 stable cell line; and Joseph Brzostowski for help in live-cell imaging. This work is supported by intramural funding from the National Institute of Allergy and Infectious Diseases, National Institutes of Health.

REFERENCES

- Aderem A, Underhill DM (1999). Mechanisms of phagocytosis in macrophages. *Annu Rev Immunol* 17, 593–623.
- Amulic B, Cazalet C, Hayes GL, Metzler KD, Zychlinsky A (2012). Neutrophil function: from mechanisms to disease. *Annu Rev Immunol* 30, 459–489.
- Beck G, Habicht GS (1996). Immunity and the invertebrates. *Sci Am* 275, 60–63, 66.
- Berton G, Mocsai A, Lowell CA (2005). Src and Syk kinases: key regulators of phagocytic cell activation. *Trends Immunol* 26, 208–214.
- Bestebroer J, De Haas CJ, Van Strijp JA (2010). How microorganisms avoid phagocyte attraction. *FEMS Microbiol Rev* 34, 395–414.
- Bjerknes R, Bassøe C-F (1984). Phagocyte C3-mediated attachment and internalization: flow cytometric studies using a fluorescence quenching technique. *Blut* 49, 315–323.
- Bufe B, Zufall F (2016). The sensing of bacteria: emerging principles for the detection of signal sequences by formyl peptide receptors. *Biomol Concepts* 7, 205–214.
- Canton J, Neculai D, Grinstein S (2013). Scavenger receptors in homeostasis and immunity. *Nat Rev Immunol* 13, 621–634.
- Colucci-Guyon E, Tinevez JY, Renshaw SA, Herbomel P (2011). Strategies of professional phagocytes in vivo: unlike macrophages, neutrophils engulf only surface-associated microbes. *J Cell Sci* 124, 3053–3059.
- Cosson P, Soldati T (2008). Eat, kill or die: when amoeba meets bacteria. *Curr Opin Microbiol* 11, 271–276.
- DeVries ME, Kelvin AA, Xu L, Ran L, Robinson J, Kelvin DJ (2006). Defining the origins and evolution of the chemokine/chemokine receptor system. *J Immunol* 176, 401–415.
- Freeman SA, Grinstein S (2014a). Phagocytosis: receptors, signal integration, and the cytoskeleton. *Immunol Rev* 262, 193–215.
- Freeman SA, Grinstein S (2014b). Phagocytosis: receptors, signal integration, and the cytoskeleton. *Immunol Rev* 262, 193–215.
- Futosi K, Mocsai A (2016). Tyrosine kinase signaling pathways in neutrophils. *Immunol Rev* 273, 121–139.
- Gallagher R, Collins S, Trujillo J, McCredie K, Ahearn M, Tsai S, Metzgar R, Aulakh G, Ting R, Ruscetti F, et al. (1979). Characterization of the continuous, differentiating myeloid cell line (HL-60) from a patient with acute promyelocytic leukemia. *Blood* 54, 713–733.
- Gao JL, Lee EJ, Murphy PM (1999). Impaired antibacterial host defense in mice lacking the N-formylpeptide receptor. *J Exp Med* 189, 657–662.
- Goldberg JM, Manning G, Liu A, Fey P, Pilcher KE, Xu Y, Smith JL (2006). The dictyostelium kinome—analysis of the protein kinases from a simple model organism. *PLoS Genet* 2, e38.
- Hanke JH, Gardner JP, Dow RL, Changelian PS, Brissette WH, Weringer EJ, Pollok BA, Connelly PA (1996). Discovery of a novel, potent, and Src family-selective tyrosine kinase inhibitor. Study of Lck- and FynT-dependent T cell activation. *J Biol Chem* 271, 695–701.
- Hartt JK, Barish G, Murphy PM, Gao JL (1999). N-formylpeptides induce two distinct concentration optima for mouse neutrophil chemotaxis by differential interaction with two N-formylpeptide receptor (FPR) subtypes. Molecular characterization of FPR2, a second mouse neutrophil FPR. *J Exp Med* 190, 741–747.
- Hishikawa T, Cheung JY, Yelamarty RV, Knutson DW (1991). Calcium transients during Fc receptor-mediated and nonspecific phagocytosis by murine peritoneal macrophages. *J Cell Biol* 115, 59–66.
- Hoeller O, Toettcher JE, Cai H, Sun Y, Huang CH, Freyre M, Zhao M, Devreotes PN, Weiner OD (2016). Gbeta regulates coupling between actin oscillators for cell polarity and directional migration. *PLoS Biol* 14, e1002381.
- Huang CH, Tang M, Shi C, Iglesias PA, Devreotes PN (2013). An excitable signal integrator couples to an idling cytoskeletal oscillator to drive cell migration. *Nat Cell Biol* 15, 1307–1316.
- Isik N, Brzostowski JA, Jin T (2008). An Elmo-like protein associated with myosin II restricts spurious F-actin events to coordinate phagocytosis and chemotaxis. *Dev Cell* 15, 590–602.

- Jiao X, Zhang N, Xu X, Oppenheim JJ, Jin T (2005). Ligand-induced partitioning of human CXCR1 chemokine receptors with lipid raft microenvironments facilitates G-protein-dependent signaling. *Mol Cell Biol* 25, 5752–5762.
- Jin T, Xu X, Hereld D (2008). Chemotaxis, chemokine receptors and human disease. *Cytokine* 44, 1–8.
- Kovacs M, Nemeth T, Jakus Z, Sitaru C, Simon E, Futosi K, Botz B, Helyes Z, Lowell CA, Mocsai A (2014). The Src family kinases Hck, Fgr, and Lyn are critical for the generation of the in vivo inflammatory environment without a direct role in leukocyte recruitment. *J Exp Med* 211, 1993–2011.
- Kwon JY, Seo SG, Heo Y-S, Yue S, Cheng J-X, Lee KW, Kim K-H (2012). Piceatannol, natural polyphenolic stilbene, inhibits adipogenesis via modulation of mitotic clonal expansion and insulin receptor-dependent insulin signaling in early phase of differentiation. *J Biol Chem* 287, 11566–11578.
- Lammermann T, Afonso PV, Angermann BR, Wang JM, Kastnermuller W, Parent CA, Germain RN (2013). Neutrophil swarms require LTB4 and integrins at sites of cell death in vivo. *Nature* 498, 371–375.
- Li X, He S, Zhou X, Ye Y, Tan S, Zhang S, Li R, Yu M, Jundt MC, Hidebrand A, et al. (2016). Lyn delivers bacteria to lysosomes for eradication through TLR2-initiated autophagy related phagocytosis. *PLoS Pathog* 12, e1005363.
- Liu M, Chen K, Yoshimura T, Liu Y, Gong W, Wang A, Gao JL, Murphy PM, Wang JM (2012). Formylpeptide receptors are critical for rapid neutrophil mobilization in host defense against *Listeria monocytogenes*. *Sci Rep* 2, 786.
- Lu T, Porter AR, Kennedy AD, Kobayashi SD, DeLeo FR (2014). Phagocytosis and killing of *Staphylococcus aureus* by human neutrophils. *J Innate Immun* 6, 639–649.
- Majumdar R, Tavakoli Tameh A, Parent CA (2016). Exosomes mediate LTB4 release during neutrophil chemotaxis. *PLoS Biol* 14, e1002336.
- Manahan CL, Iglesias PA, Long Y, Devreotes PN (2004). Chemoattractant signaling in *dictyostelium discoideum*. *Annu Rev Cell Dev Biol* 20, 223–253.
- Mangmool S, Kurose H (2011). G(i/o) protein-dependent and -independent actions of pertussis toxin (PTX). *Toxins (Basel)* 3, 884–899.
- Maniak M, Rauchenberger R, Albrecht R, Murphy J, Gerisch G (1995). Corin involved in phagocytosis: dynamics of particle-induced relocalization visualized by a green fluorescent protein Tag. *Cell* 83, 915–924.
- Michl J, Pieczonka MM, Unkless JC, Silverstein SC (1979). Effects of immobilized immune complexes on Fc- and complement-receptor function in resident and thioglycollate-elicited mouse peritoneal macrophages. *J Exp Med* 150, 607–621.
- Millius A, Weiner OD (2009). Chemotaxis in neutrophil-like HL-60 cells. *Methods Mol Biol* 571, 167–177.
- Nathan C (2006). Neutrophils and immunity: challenges and opportunities. *Nat Rev Immunol* 6, 173–182.
- Nunes P, Demaurex N (2010). The role of calcium signaling in phagocytosis. *J Leukoc Biol* 88, 57–68.
- Pan M, Neilson MP, Grunfeld AM, Cruz P, Wen X, Insall RH, Jin T (2018). A G-protein-coupled chemoattractant receptor recognizes lipopolysaccharide for bacterial phagocytosis. *PLoS Biol* 16, e2005754.
- Pan M, Xu X, Chen Y, Jin T (2016). Identification of a chemoattractant G-protein-coupled receptor for folic acid that controls both chemotaxis and phagocytosis. *Dev Cell* 36, 428–439.
- Pan P, Hall EM, Bonner JT (1972). Folic acid as second chemotactic substance in the cellular slime moulds. *Nat New Biol* 237, 181–182.
- Pan P, Hall EM, Bonner JT (1975). Determination of the active portion of the folic acid molecule in cellular slime mold chemotaxis. *J Bacteriol* 122, 185–191.
- Ricklin D, Reis ES, Mastellos DC, Gros P, Lambris JD (2016). Complement component C3—the “Swiss Army Knife” of innate immunity and host defense. *Immunol Rev* 274, 33–58.
- Rougerie P, Miskolci V, Cox D (2013). Generation of membrane structures during phagocytosis and chemotaxis of macrophages: role and regulation of the actin cytoskeleton. *Immunol Rev* 256, 222–239.
- Sada K, Takano T, Yanagi S, Yamamura H (2001). Structure and function of Syk protein-tyrosine kinase. *J Biochem* 130, 177–186.
- Shelef MA, Tauzin S, Huttenlocher A (2013). Neutrophil migration: moving from zebrafish models to human autoimmunity. *Immunol Rev* 256, 269–281.
- Sjostrom M, Wold S, Wieslander A, Rilfors L (1987). Signal peptide amino acid sequences in *Escherichia coli* contain information related to final protein localization. A multivariate data analysis. *EMBO J* 6, 823–831.
- Stenfeldt AL, Karlsson J, Wenneras C, Bylund J, Fu H, Dahlgren C (2007). Cyclosporin H, Boc-MLF and Boc-FLFLF are antagonists that preferentially inhibit activity triggered through the formyl peptide receptor. *Inflammation* 30, 224–229.
- Stuart LM, Ezekowitz RA (2008). Phagocytosis and comparative innate immunity: learning on the fly. *Nat Rev Immunol* 8, 131–141.
- Sumimoto H (2008). Structure, regulation and evolution of Nox-family NADPH oxidases that produce reactive oxygen species. *FEBS J* 275, 3249–3277.
- Swanson JA (2008). Shaping cups into phagosomes and macropinosomes. *Nat Rev Mol Cell Biol* 9, 639–649.
- Underhill DM, Goodridge HS (2012). Information processing during phagocytosis. *Nat Rev Immunol* 12, 492–502.
- Underhill DM, Gordon S, Imhof BA, Nunez G, Bousso P (2016). Elie Metchnikoff (1845–1916): celebrating 100 years of cellular immunology and beyond. *Nat Rev Immunol* 16, 651–656.
- Underhill DM, Ozinsky A (2002). Phagocytosis of microbes: complexity in action. *Annu Rev Immunol* 20, 825–852.
- Wenzel-Seifert K, Seifert R (1993). Cyclosporin H is a potent and selective formyl peptide receptor antagonist. Comparison with N-t-butoxycarbonyl-L-phenylalanyl-L-leucyl-L-phenylalanyl-L-leucyl-L-phenylalanine and cyclosporins A, B, C, D, and E. *J Immunol* 150, 4591–4599.
- Wood WB Jr, Smith MR, Watson B (1946a). Surface phagocytosis—its relation to the mechanism of recovery in pneumococcal pneumonia. *Science* 104, 28–29.
- Wood WB, Smith MR, Watson B (1946b). Studies on the mechanism of recovery in pneumococcal pneumonia: iv. the mechanism of phagocytosis in the absence of antibody. *J Exp Med* 84, 387–402.
- Woodham EF, Paul NR, Tyrrell B, Spence HJ, Swaminathan K, Scribner MR, Giampazolias E, Hedley A, Clark W, Kage F, et al. (2017). Coordination by Cdc42 of actin, contractility, and adhesion for melanoblast movement in mouse skin. *Curr Biol* 27, 624–637.
- Ye RD, Boulay F, Wang JM, Dahlgren C, Gerard C, Parmentier M, Serhan CN, Murphy PM (2009). International union of basic and clinical pharmacology. LXXIII. Nomenclature for the formyl peptide receptor (FPR) family. *Pharmacol Rev* 61, 119–161.